

A survey of Classical Methods and New Trends in Hyperspectral Unmixing

Anitha.K¹, Nishanth Augustine²

Department of Electronics and Communication Engineering, LBS College of Engineering, Kasaragod, India^{1,2}

Abstract: A break through development in remote sensing is Hyperspectral Imaging. Imaging Spectrometers, often referred to as hyperspectral cameras (HSCs) are used for hyperspectral imaging and they acquire images with higher spectral resolution than multispectral cameras. Due to low spatial resolution of HSCs, spectra measured by HSCs are mixtures of spectra of materials in a scene and each pixel is assumed to be a mixture of few materials, called endmembers. This necessitates unmixing which involves estimating the number of endmembers, their spectral signatures and their abundances at each pixel. Various algorithms like HYSIME, VCA, DECA, NMF, N-Finder were introduced for hyperspectral unmixing. A sparse regression scheme based on compressive sensing is also used for identifying pure form of pixels of a scene. This approach reduces the number of endmembers needed to represent the data and provides more robust solutions. A collaborative Sparse Regression method is also developed which can be implemented in parallel nature and thus improves the speed of operation and accuracy. In this paper a brief study of various unmixing algorithms were presented along with a comparison of their performance.

Keywords: Hyperspectral Imaging, Hyperspectral Unmixing (HU), endmembers, Compressive sensing, Hysime, VCA, DECA, Spectral library.

I. INTRODUCTION

Remote Sensing is defined as the science and technology by which the characteristics of objects of interest can be identified, measured or analysed without direct contact. Electromagnetic radiation which is reflected or emitted from an object is the usual source of remote sensing data. However any media such as gravity or magnetic fields can be utilized in remote sensing.

Hyperspectral images (HSI) are taken by satellites such that each pixel records an area of geographical information in form of electromagnetic spectral reflectance. Hyperspectral imaging sensors collect two dimensional spatial images over many contiguous bands of high spectral resolution covering the visible, near-infrared, and shortwave infrared spectral bands [18,19]. Since an ordinary image takes two dimensions, an HSI requires the third dimension in order to store spectral data for every pixels.

HSCs can be built to function in many regions of the electromagnetic spectrum.

Hyperspectral unmixing is the decomposition of the pixel spectrum into a collection of constituent spectra, or spectral signatures, and their corresponding abundance fractions, occasionally termed sources, indicating the proportion of each endmember present in the pixel [15].

Unmixing is a challenging, ill-posed inverse problem because of model inaccuracies, observation noise, environmental conditions, endmember variability, and data set size. Due to low spatial resolution of HSCs, microscopic material mixing, and multiple scattering, spectra measured by HSCs are mixtures of spectra of materials in a scene. Thus, accurate estimation requires unmixing.

This paper is organized in to 4 sections. Section-II describes the basis of HSI and unmixing. Section-III introduces various unmixing algorithms like Hysime, VCA, DECA and their corresponding results. Section IV discusses the experimental results. Conclusion is described in section V.

II. HYPERSECTRAL IMAGING

A. Hyperspectral Data Acquisition

The science of remote sensing has advanced over the recent past by using increasingly capable sensors. The development of an extremely powerful class of Earth remote sensing instruments has improved the capability of ground-based data collection in the fields of agriculture, geography, geology, mineral identification, detection [7,19], and classification [3,17].

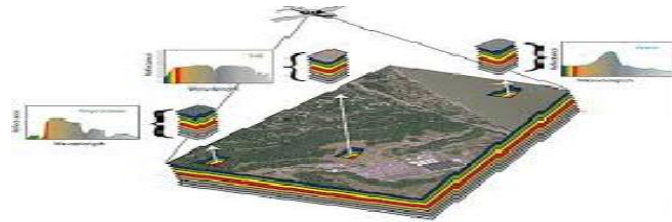


Fig.1 Principle of hyperspectral data acquisition

The AVIRIS [21], Probe-1 [8], and Hymap [23] instruments perform the collection of data in a whisk-broom mode to the cross-track direction by mechanical scanning and in the along-track direction by movement of the platform. Hyperion [29] and HyDICE [25] instruments use a push-broom imaging sensor, which acquires data in a cross-track line without any mechanical scanning. The digital data is produced by an analog to digital converter, which samples the radiance measured in each spectral channel with a given radiometric resolution. Figure 1(a) illustrates the principles involved in the hyperspectral data acquisition. The spatially and spectrally sample information of the ground surface can be described by a three dimensional structure, referred to as a data cube.

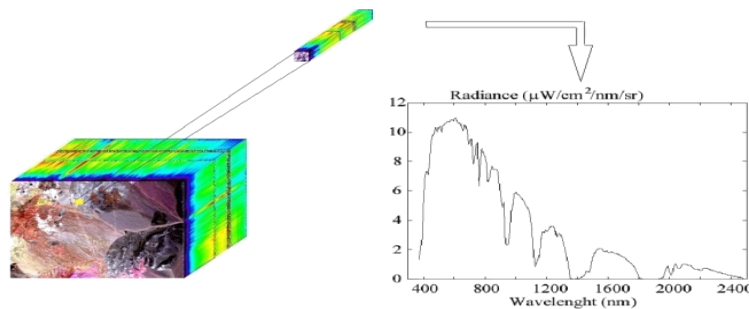


Fig.2 Hyperspectral data cube and pixel radiance example

Figure.2 shows an example of such a data cube and the radiance of a pixel vector as a function of the wavelength. The ground pixel size varies from meters to tens of meters depending on the altitude of the platform and on the instantaneous field of view (IFOV) of the sensor. The information content of hyperspectral images with thousands of pixels and hundreds of channels allows us to remotely identify ground materials, based on their spectral signature, and to perform land characterization based on the abundance of each material.

B. Fundamentals of Unmixing

Very often, the spatial portion occupied by a substance is smaller than the ground pixel size (tens of meters). As a result, the signal read by the sensor from a given spatial element of resolution and at a given spectral band is a mixing of components originated from the constituent substances, termed endmembers, located at that element of resolution [18]. In this situation, the scattered energy is a mixing of the endmember spectrum [12,24]. Depending on the mixing scales at each pixel, the observed mixture is either linear or nonlinear [16]. The linear mixing model holds approximately when the mixing scale is macroscopic [28] and there is negligible interaction among distinct endmembers [9,11]. The nonlinear model holds when the mixing scale is microscopic (i.e., intimate mixtures) [30]. Figure 1.3(b) illustrates an intimate mixture, yielding a nonlinear scenario. The linear model assumes negligible interaction among distinct endmembers [9]. The nonlinear model assumes that incident solar radiation is scattered by the scene through multiple bounces involving several endmembers [6]. Very often, the effects of multiple scattering are assumed to be negligible and thus the linear model is adopted [20].

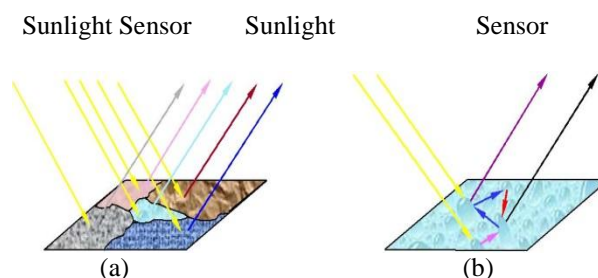


Fig. 3 Illustration of a pixel: (a) linear mixture (macroscopic mixing scale); (b): nonlinear mixture (intimate mixture).

The most common steps to unmix hyperspectral data are illumination and atmospheric effects, due to these effects the radiance acquired by hyperspectral sensors cannot be directly compared with a digital spectral library or even with other radiance data sets. This comparison is made possible by the atmospheric correction, which transforms the radiance spectra into reflectance. This operation accounts for solar spectrum, sensor and sun directions, path radiance, secondary illumination, and shadowing. The second operation, data reduction, is a consequence of the fact that the number of endmembers present in the scene is usually much smaller than the number of bands of a hyperspectral data set. This operation has a great impact since it reduces the amount of data, implying computational savings in the unmixing step, and it improves the signal-to-noise ratio (SNR). The third operation, spectral unmixing, usually embodies two steps: endmember determination and inversion. The first step estimates the signatures of the distinct endmembers present in the scene. The second step estimates the abundance fractions of each endmember. To conduct the hyperspectral unmixing operation, a mixture model must be adopted to describe how the constituent endmembers and how the atmosphere scatters the sun light at a given pixel. This process is addressed in the next section. A lot of algorithms like HYSIME, VCA, DECA, were introduced for hyperspectral unmixing. Hysime for signal subspace identification, VCA for endmember extraction, DECA for abundance fraction estimation through dirichlets distributions, n-finder for identifying pure pixel in a scene likewise above algorithms using Hyperspectral Unmixing. By using Sparse regression scheme, able to identify pure form of pixels in that scene.

III. UNMIXING ALGORITHMS

A. HYSIME: An Hyperspectral Signal Subspace Estimator

The method is based on a mean squared error (MSE) approach to determine the signal subspace in hyperspectral imagery. HySime is an eigen decomposition based method; it first estimates the signal and noise correlations matrices, then it selects the subset of eigenvalues that best represents the signal subspace in the least square sense.

The noise estimation, a necessary step in the HySime algorithm, is based on the multiple regression theory and exploits the high correlation existing between contiguous hyperspectral bands. This method has been optimized to reduce the computational complexity. Parts of HySime were published in [4,5].

(a) Dimensionality reduction:

Dimensionality reduction has been approached in many ways. Band selection or band extraction, as the name suggests, exploits the high correlation existing between adjacent bands to select a few spectral components among those with higher SNR [2,13]. The signal subspace methods can be classified either as global or local [14]. The global methods estimate the signal subspace using the complete data set. Projection techniques, which are usually used in the global approaches, seek for the best subspace to project data by minimizing an objective function.

(b) Signal Subspace Estimation:

This section introduces formally a new method to estimate the hyperspectral signal subspace termed hyperspectral signal identification by minimum error (HySime). The method starts by estimating the signal and the noise correlation matrices and then it selects the subset of eigenvectors that best represents the signal subspace in the minimum mean squared error sense.

The application of this criterion leads to the minimization of a two-term objective function. One term corresponds to the power of the signal projection error and is a decreasing function of the subspace dimension; the other term corresponds to the power of the noise projection and is an increasing function of subspace dimension.

(c) Noise Estimation:

Noise estimation is a classical problem in data analysis and particularly in remote sensing. Arguably, in hyperspectral imagery, the simplest noise estimation procedure is the shift difference method, also denominated as nearest neighbor difference (NND) [10]. This approach assumes that noise samples taken from adjacent pixels are independent and have the same statistics, but the signal component is practically equal. To obtain meaningful noise estimates, the shift difference method shall be applied in homogeneous areas rather than on the entire image.

ALGORITHM 1: Noise Estimation

1. INPUT $H \equiv [h_1, h_2, \dots, h_N]$
2. $Z = H^T, K := (Z^T Z); K' := K^{-1}$
3. For $i := 1$ to L do
4. $B_i := ([k']_{\partial i, \partial i} - [K']_{\partial i, i} [K']_{i, \partial i} / [K']_{i, i}) [K]_{\partial i, i}$
{Note that $\partial i = 1, \dots, i-1, i+1, \dots, L$ }
5. $\hat{\xi}_i := Z_i - Z_{\partial i} B_i$; End for; Output $\hat{\xi}$; { $\hat{\xi}$ is a $N \times L$ matrix with a estimated noise }.

The pseudo code for the noise estimation is shown above Algorithm .Symbol $[K]_{\hat{\delta}_i, \hat{\delta}_i}$ denotes the matrix obtained from $[K]$ by deleting the i th row and the i th column, $[K]_{i, \hat{\delta}_i}$ denotes the i th row of $[K]_{\hat{\delta}_i, \hat{\delta}_i}$, and $[K]_{\hat{\delta}_i, i}$ denotes $[K]_{\hat{\delta}_i, \hat{\delta}_i}^T$. Steps 2 and 3 compute matrix $[K] = Z^T Z$ and its inverse, respectively. Steps 5 & 6 estimates, respectively, the regression vector B_i the noise $\hat{\xi}_i$, for each $i=1, \dots, L$. Brief details about this algorithm as shown in paper[31].

ALGORITHM 2: HYSIME

1. INPUT $H \equiv [h_1, h_2, \dots, h_N]$; $K_r \equiv (RR^T)/N$;
2. $K := \frac{1}{N} \sum i(\hat{n}_i \hat{n}_i^T)$; $\{K_n$ is the noise correlation matrix estimates}
3. $K_x := \frac{1}{N} \sum i((r_i - \hat{n}_i)(r_i - \hat{n}_i^T))$; $\{K_x$ is the signal correlation matrix estimate}; $U_k := E_k E_k^T$: {where E_k are eigen vectors of K_x }.
4. $K := \arg \min_k \{tr(U_k^{\perp} K_r) + 2tr(U_k K_n)\}$

The pseudo code for HySime is shown above Algorithm. HySime inputs are the spectral observed vectors and the sample correlation matrix K_r . Step 2 estimates the noise correlation matrix K_n . Step 3 estimates the signal correlation matrix K_x . Step 4 and 5 calculate the eigenvectors of the signal correlation matrix and the mean squared error function. The minimizer of this function is the estimated signal subspace dimension, K . The main advantage of Algorithm 2 is that the computation of $[K]$ and of $K^{-1} = [K]^{-1}$ are out of the loop for. Thus, the computational complexity, i.e., the number of floating point operations (flops), of Algorithm 2 is substantially lower than that of an algorithm implementing the multiple regression without any assumptions. This method has two weaknesses: first, it assumes that adjacent pixels have the same signal information, which is not valid in most hyperspectral data sets; second, to improve the noise estimation, a supervised selection of homogeneous areas must be carried out.

B. VERTEX COMPONENT ANALYSIS: A FAST ALGORITHM TO UNMIX HYPERSPECTRAL DATA

Hyperspectral vectors are mixtures of the spectral signatures of the endmembers present in the scene. Linear spectral mixture analysis, or linear unmixing, aims at estimating the number of endmembers, their spectral signatures, and their abundance fractions. Usually, this task embodies two steps: endmember extraction to determine the spectral signatures of endmembers followed by inversion to estimate the abundance fractions of each endmember. Brief details about this algorithm as shown in paper[32].

The algorithm exploits two facts:

- (i) the endmembers are the vertices of a simplex and
- (ii) the affine transformation of a simplex is also a simplex. Principle Component Analysis

ALGORITHM 3: VCA

1. INPUT $H \equiv [h_1, h_2, \dots, h_N]$
2. $P := \text{Hysime}(H)$; {the number of endmembers estimated by Hysim algorithm}
3. $\text{SNR}_{th} := 15 + 10 \log_{10}(p) \text{dB}$;
4. If $\text{SNR} > \text{SNR}_{th}$, then ; $d := p$;
5. $X := U_d^T H$; $\{U_d$ obtained by SVD}
6. $U := \text{mean}(X)$; $\{u$ is a $1 \times d$ vector}
7. $[Y]_j := [X]_j / ([X]_j^T u)$; {projective projection}
8. Else; $d := p-1$;
9. $[X] := U_d^T ([H]_j - \bar{r})$; $\{U_d$ is obtained by PCA}
10. $K := \arg \max_{j=1, \dots, N} \|[X]_{:,j}\|$;
11. $K := [k|k| \dots |k]$; $\{k$ is a $1 \times N$ vector}
12. $Y := \frac{X}{k}$; End if
13. $A := [e_u | 0 | \dots | 0]$; $\{e_u := [0, \dots, 0, 1]^T$ and A is a $p \times p$ auxiliary matrix}
14. For $i := 1$ to p do
15. $W = \text{randn}(0, I_p)$ { w is a zero mean random gaussian vector of covariance I_p }
16. $f := \frac{(I_p - AA^{\#})W}{\|(I_p - AA^{\#})W\|}$; $\{f$ is a vector orthonormal to subspace spanned by $[A]_{:,1:i}\}$
17. $v := f^T Y$; $k := \arg \max_{j=1, \dots, N} \|[v]_{:,j}\|$; {find the projection extreme};
18. $[A]_{:,i} := [Y]_{:,k}$;
19. $[\text{indice}]_i := k$ {stores the pixel index};
20. End for; if $\text{SNR} > \text{SNR}_{th}$ then

21. $M := U_d[X]_{:, \text{indice}} ; \{ \hat{M} \text{ is a } L \times P \text{ estimated mixing matrix} \}$
22. Else; $M := U_d [X]_{:, \text{indice} + \bar{r}} ; \{ M \text{ is a } L \times p \text{ estimated mixing matrix} \}$
- 29: end if

C. DEPENDENT COMPONENT ANALYSIS

This presents a new direction to blindly unmix hyperspectral data, termed dependent component analysis (DECA), where abundance fractions are modeled by a mixture of Dirichlet densities, thus enforcing source non negativity and additivity constraints. DECA is in the vein of works [1,22] replacing independent sources represented by MOGs with mixtures of Dirichlet (MODs) sources. Compared with the geometric-based approaches, the advantage of DECA is that there is no need to have pure pixels in the observations. Brief details about this algorithm as shown in paper[33].

ALGORITHM 4: DECA

1. initialize T, \hat{W}, θ and L_{best}
2. while $L_N - L_{\text{BEST}} > \text{threshold}$ do
3. $\hat{s} := \hat{W}^{(0)} X$; For $q := 1$ to K do
4.
$$D\left(\hat{s} \mid \hat{\theta}_q^{(T)}\right) := \frac{\Gamma\left(\sum_{j=1}^p \hat{\theta}_{qj}^{(T)}\right)}{\prod_{j=1}^p \Gamma\left(\hat{\theta}_{qj}^{(T)}\right)} \prod_{j=1}^p \hat{s}_j^{\hat{\theta}_{qj}^{(T)} - 1}$$
;
5.
$$\beta_q^{(t)} := \frac{\hat{\varepsilon}_q^{(t)} D\left(\hat{s} \mid \hat{\theta}_q^{(t)}\right)}{\sum_{i=1}^K \hat{\varepsilon}_i^{(t)} D\left(\hat{s} \mid \hat{\theta}_i^{(t)}\right)}$$
;
6. $\hat{\varepsilon}_q^{(t)} := T[\beta_q^{(t)}]$; end for; for $j := 1$ to p do
7.
$$\theta_{\text{aux}_{qj}} := \text{psi}^{-1}\left(\text{psi}\left(\sum_{i=1}^p \hat{\theta}_{qi}^{(t)}\right) + \frac{T\left[\beta_q^{(t)} \log \hat{s}_j^{(t)}\right]}{T[\beta_q^{(t)}]}\right)$$
;
8.
$$\frac{\partial Q}{\partial w_j} := T\left[\sum_{q=1}^K \left(\beta_q^{(t)} \frac{\hat{\theta}_{qj}^{(t)} - 1}{\hat{s}_j} X^T - \beta_q^{(t)} \frac{\hat{\theta}_{qp}^{(t)} - 1}{\hat{s}_p} X^T\right)\right] + \left[\hat{W}^{-T}\right]_j - \left[\hat{W}^{-T}\right]_p$$
;
9. end for; $W_{\text{aux}} := \hat{W}^{(t)} + T \frac{\partial Q}{\partial W}$;
10. $L_N := T\left[\log \sum_{q=1}^K \hat{\varepsilon}_q^{(t)} D\left(s \mid \theta_{\text{aux}_q}\right)\right] + \log(|\det W_{\text{aux}}|)$;
11. if $L_{\text{best}} < L_N$ then; $L_{\text{best}} = L_N$; $\hat{W}^{(t+1)} := W_{\text{aux}}$;
12. $\hat{\theta}^{(t+1)} := \theta_{\text{aux}}$; increment T ; else; decrement T ; end if ; End while

The Algorithm 4 presents the pseudo code aimed at the maximization. It implements a cyclic maximizer algorithm, which splits the estimation of W and θ into block maximization operations. The estimation of W uses a gradient ascendant method with adaptative steps. The estimation of θ is based on the algorithm described and the resulting scheme replacing at independent sources, represented by MOGs with mixture of Dirichlet sources.

D. SPARSE REGRESSION:

Linear spectral unmixing is a popular tool in remotely sensed hyperspectral data interpretation. The unmixing problem can also be approached in semi-supervised fashion, i.e. by assuming that the observed image signatures can be expressed in the form of linear combinations of a number of pure spectral signatures known in advance (e.g. spectra collected on the ground by a field spectro-radiometer). In practice, unmixing is a combinatorial problem which calls for efficient linear sparse regression techniques based on sparsity-inducing regularizers, since the number of endmembers participating in a mixed pixel is usually very small compared with the dimensionality and availability of spectral libraries. Linear sparse regression is an area of very active research with strong links to compressed sensing, basis pursuit, basis pursuit denoising, and matching pursuit. Furthermore, we provide a comparison of several available and new linear sparse regression algorithms with the ultimate goal of analyzing their potential in solving the spectral

unmixing problem by resorting to available spectral libraries. Results by the NASA Jet Propulsion Laboratory’s Airborne Visible Infra-Red Imaging Spectrometer (AVIRIS) and spectral libraries publicly available from U.S. Geological Survey (USGS)¹, indicate the potential of sparse regression techniques in the task of accurately characterizing mixed pixels using library spectra. This opens new perspectives for spectral unmixing, since the abundance estimation process no longer depends on the availability of pure spectral signatures in the input data nor on the capacity of a certain endmember extraction algorithm to identify such pure signatures. $A \in \mathbb{R}^{L \times m}$, where L and m are the number of spectral bands and the number of materials in the library, respectively. All libraries herein considered correspond to under-determined systems, i.e., $L < m$. With the aforementioned assumptions in mind, let $x \in \mathbb{R}^m$ denote the fractional abundance vector with regards to the library A . As usual, we say that x is a k -sparse vector if it has at most k components different from zero. With these definitions in place, we can now write our Sparse regression problem as:

$$\min_x \|x\|_0 \text{ subject to } \|y - Ax\|_2 \leq \delta, x \geq 0, 1^T x = 1, \quad (1)$$

where $\|x\|_0$ denotes the number of non-zero components of x and $\delta \geq 0$ is the error tolerance due to noise and modelling errors. A solution of problem (1), if any, belongs to the set of sparsest signals belonging to the $(m-1)$ probability simplex satisfying error tolerance inequality $\|y - Ax\|_2 \leq \delta$. Prior to addressing problem (1), we consider a series of simpler related problems..

(a). Collaborative Sparse Regression:

collaborative sparse regression improves hyperspectral unmixing by taking advantage of the fact that the number of endmembers in a given hyperspectral scene is generally low and all the observed pixels are generated by the same set of endmembers. These aspects are addressed through a new algorithm called CLSUnSAL which is able to accurately infer the abundance fractions in both simulated and real environments.

The ADMM (Alternating Direction Method of Multipliers) algorithm for the formulation finds the set of pixels defining the largest volume by inflating a simplex inside the data.

ALGORITHM: ADMM

1. Initialization: set $k=0$, choose $\mu > 0$, $U^{(0)}$, $V^{(0)}$, $D^{(0)}$.
2. repeat:
3. $U^{(k+1)} \leftarrow \arg \min_U L(U^{(k)}, V^{(k)}, D^{(k)})$
4. $V^{(k+1)} \leftarrow \arg \min_V L(U^{(k+1)}, V^{(k)}, D^{(k)})$
5. $D^{(k+1)} \leftarrow D^{(k)} - GU^{(k+1)} - BV^{(k+1)}$
6. until some stopping criterion is satisfied.

E. NMF: Non-Negative Matrix Factorization:

Hyperspectral unmixing is therefore used to decompose received spectral reflectance of each pixel into a sum of reflectance (also called endmembers) weighted by the corresponding materials’ contribution (known as abundance) in that pixel [6]. These materials can be anything found from the Earth surface, which are categorized into minerals, coatings, man-made structure, plants, etc. According to U.S. Geological Survey (USGS). Since endmembers and abundance are non-negative, non-negative matrices can represent HSI endmembers and abundance. Therefore the NMF process of an HU problem can be modelled as a multiplication of two non-negative matrices, $Y \approx Y^1 = A * S$ where Y , A and S represent HSI, endmember and abundance respectively. Figure 2.7 visually shows the mathematical model of NMF. It should be noted that the factorized matrices A and S have size $m \times k$ and $k \times n$ respectively, where their common size k is called model order. Its physical meaning is the total number of endmembers that exist in the HSI.

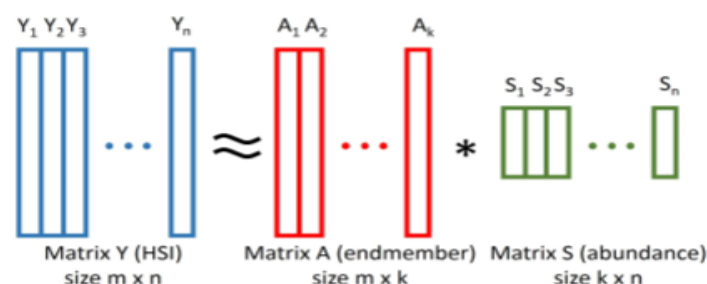


Fig 4 Illustration of Non Negative Matrix Factorization

F. N-FINDER

N-FINDER is based on the fact that in spectral dimensions, the volume defined by a simplex formed by the purest pixels is larger than any other volume defined by any other combination of pixels. This algorithm finds the set of pixels

defining the largest volume by inflating a simplex inside the data. It has been frequently used as a benchmark for new algorithms and as a basis for modification. Here opportunities for improving the algorithm exist, particularly to reduce its computational expense.

ALGORITHM: Successive N-FINDER:

1. Let p be the number of endmembers required to be generated and $\{e^{(0)}_1, \dots, e^{(0)}_p\}$ be a set of initial vectors randomly selected from the data
2. For $1 \leq j \leq p$, find $E_j^* = \arg\{\max V(e_1^*, \dots, e_{j-1}^*, e_{j+1}^{(0)}, \dots, e_p^{(0)})\}$.
3. The set of $\{e^*_1, \dots, e^*_p\}$ is the desired endmembers.

The successive volume maximization (SVMAX) is similar to VCA. The main difference concerns the way data is projected onto a direction orthogonal the subspace spanned by the endmembers already determined. VCA considers a random direction in these subspace, whereas SVMAX considers the complete subspace.

IV. EXPERIMENTAL RESULTS

The experiments were conducted on publically available USGS library data base. The images were collected from different sensors like AVIRS, HYDICE. So their spectral and spatial resolution and imaging parameters will be different. e.g., in-plane pixel size varies. Hyperspectral images collected are in JPEG format with a size of 512x512. Proposed algorithms is tested for some USGS datasets obtained from HYDICE. Following section shows our experimental results obtained while simulating the datasets. Subspace and Noise Estimation by HYSIME, Endmember Extraction by VCA and Abundance fraction by DECA.

Results for HYSIME:

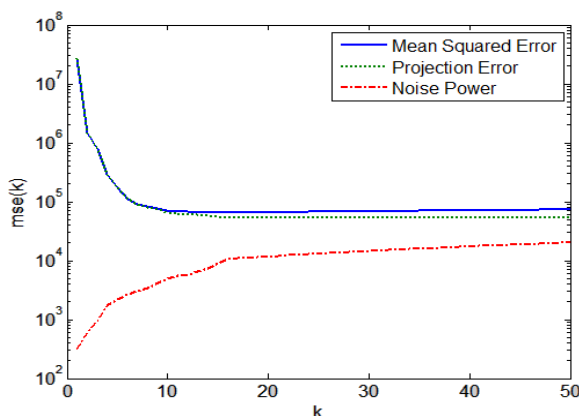


Fig. 5(a) Hysime

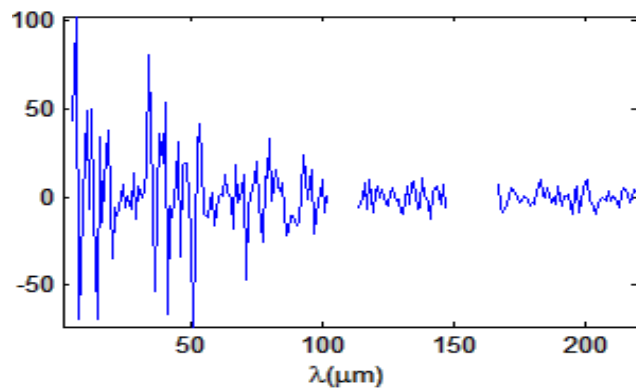


Fig. 5(b) Noise Estimates

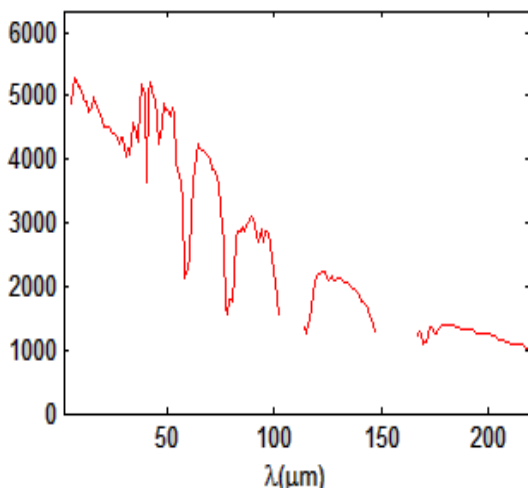


Fig.6 Pixel signature

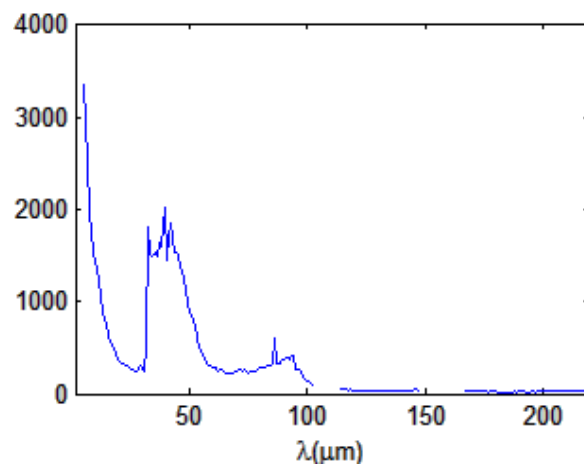


Fig.7 Diagonal of noise covariance matrix

Results for VCA:

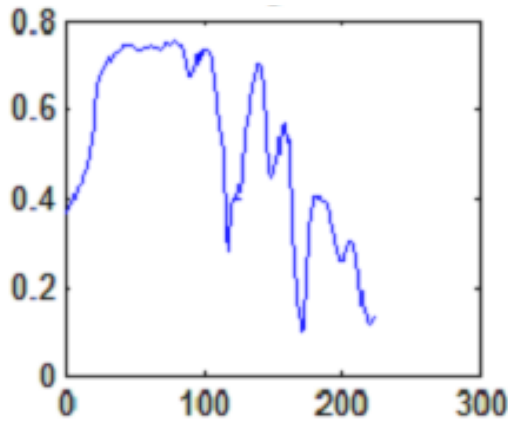


Fig.8 True Signature

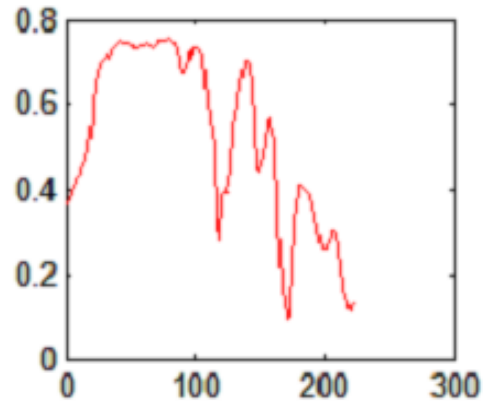


Fig.9 Abundance fraction



Fig.10 True Abundance and Signature Estimate

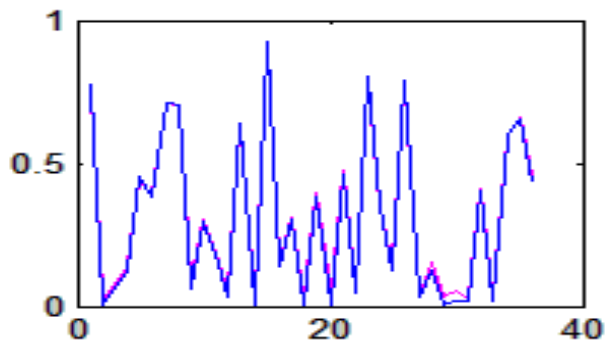


Fig.11 Line of true and estimate abundance

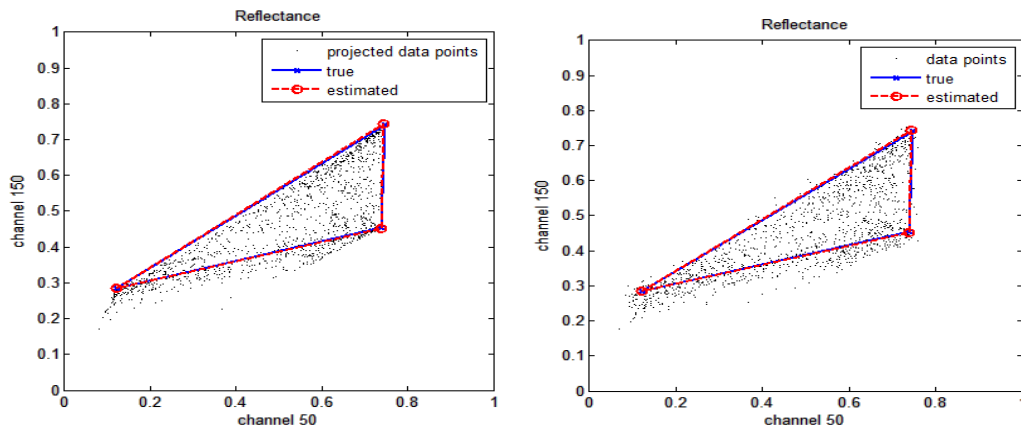


Fig. 12 data points Estimation

Results for DECA:

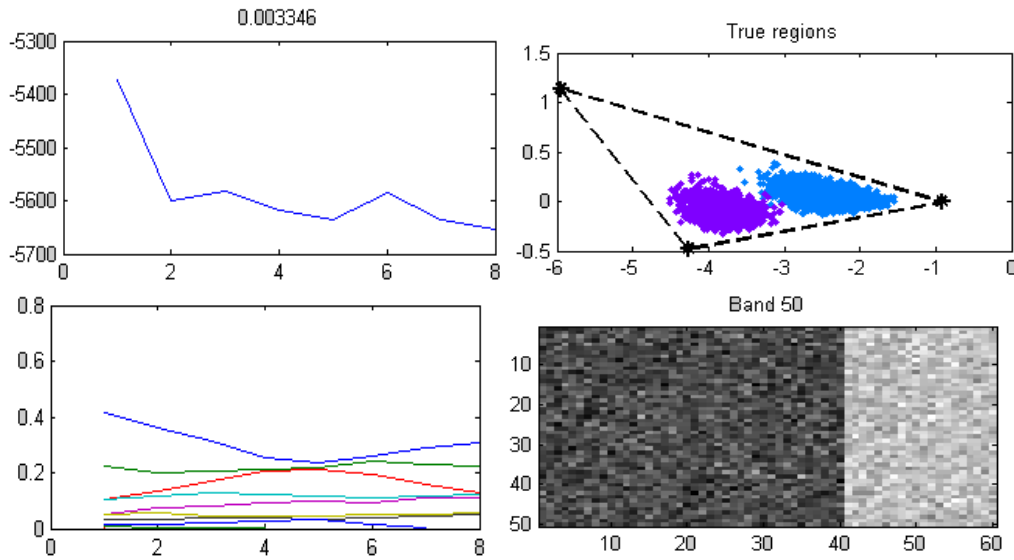


Fig.13

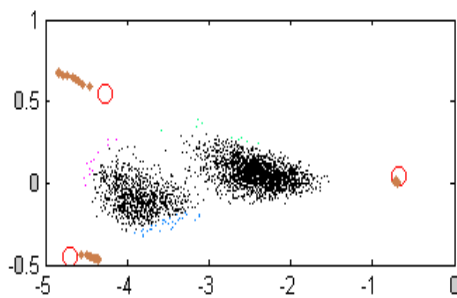


Fig.14 image regions

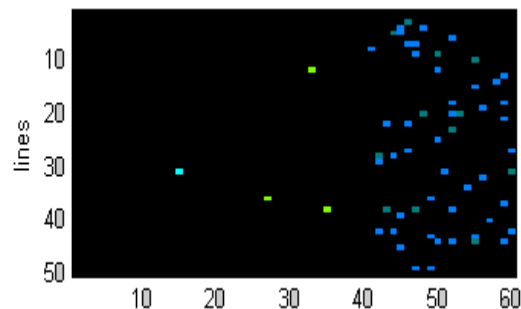


Fig.15 columns

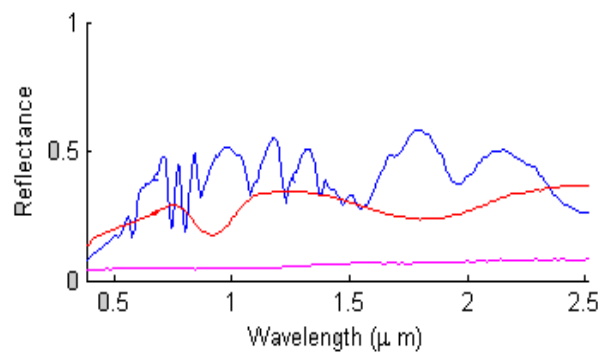


Fig.16 Signatures

V. CONCLUSION

AUnmixing hyperspectral data is the decomposition of the hyperspectral data into a collection of endmembers spectra and their corresponding abundance fractions, thus indicating the proportion of each endmember present in the scene. This paper introduces the hyperspectral signal identification by minimum error (HySime) method, which is a new mean squared error based approach to infer the signal subspace of hyperspectral data sets. Vertex Component Analysis (VCA), which is a new fast method to unmix hyperspectral data exploiting this geometric feature of hyperspectral mixtures. VCA is an unsupervised method that works with project and unprojected data. A new direction to blindly unmix hyperspectral data, termed dependent componentanalysis (DECA), using mixtures of Dirichlet (MOD) to model

abundance fractions is proposed. The method uses a expectation maximization (EM) algorithm to estimate the unmixing matrix and to estimate the Dirichlet parameters. Compared with the geometric based approaches, its advantage is that there is no need to have pure pixels in the observations.

REFERENCES

- [1] H. Attias. Independent factor analysis. *Neural Computation*, 1999.
- [2] S. De Backer, P. Kempeneers, W. Debruyne, and P. Scheunders. A band selection technique for spectral classification. *IEEE Geoscience. Remote Sensing* 2005.
- [3] J.A. Benediktsson, J.A. Palmason, and J.R. Sveinsson. Classification of hyperspectral data from urban areas based on extended morphological profiles. *IEEE Trans. Geoscience. Remote Sensing*, 2005.
- [4] Jose M. Bioucas-Dias and Jose M. P. Nascimento. Estimation of signal subspace on hyperspectral data. In Lorenzo Bruzzone, editor, *Proc. of SPIE conference on Image and Signal Processing for Remote Sensing XI*, volume 5982, 2005.
- [5] Jose M. Bioucas-Dias and Jose M. P. Nascimento. Signal and Image Processing for Remote Sensing, chapter Vertex Component Analysis: A Geometric-Based Approach to Unmix Hyperspectral Data., 2006.
- [6] C. C. Borel and S. A. Gerstl. Nonlinear spectral mixing models for vegetative and soils surface. *Rem. Sens. of the Environ.* 1994.
- [7] Chein-I Chang and D. Heinz. Subpixel spectral detection for remotely sensed images. *IEEE Trans. Geoscience Remote Sensing*, 2000.
- [8] M. Chevrier, A. Bannari, J.-C. Deguise, H. McNairn, and K. Staenz. Hyperspectral narrow wavebands for discriminating crop residue from bare soil. In *Proc. of the IEEE Int. Geoscience and Remote Sensing Symp.*, volume 4, 2002.
- [9] R. N. Clark and T. L. Roush. Reflectance spectroscopy: Quantitative analysis techniques for remote sensing applications. *J. of Geophysical Research*, 1984.
- [10] Green, M. Berman, P. Switzer, and M. D. Craig. A transformation for ordering multispectral data in terms of image quality with implications for noise removal. *IEEE Trans. Geoscience Remote Sensing*, 1988.
- [11] Hapke. Bi-direction reflectance spectroscopy. I. theory. *J. of Geophysical Research*, 1981.
- [12] Y. H. Hu, H. B. Lee, and F. L. Scarpace. Optimal linear spectral unmixing. *IEEE Trans. Geoscience. Remote Sensing*, 1999.
- [13] Rui Huang and Mingyi He. Band selection based on feature weighting for classification of hyperspectral data. *IEEE Geoscience Remote Sensing*, 2005.
- [14] K. Jain and R. C. Dubes. *Algorithms for clustering data*. Prentice Hall, N. J., 1988.
- [15] Nirmal Keshava, Jonh Kerekes, Dimitris Manolakis, and Gary Shaw. An algorithm taxonomy for hyperspectral unmixing. In *Proc. of the SPIE Aero Sense Conference on Algorithms for Multispectral and Hyperspectral Imagery VI*, volume 4049, 2000.
- [16] Nirmal Keshava and John Mustard. Spectral unmixing. *IEEE Signal Processing Magazine*, 2002.
- [17] D. Landgrebe. Hyperspectral image data analysis. *IEEE Signal Processing Magazine* 2002.
- [18] Thomas M. Lillesand, Ralph W. Kiefer, and Jonathan W. Chipman. *Remote Sensing and Image Interpretation*. John Wiley & Sons, Inc., fifth edition, 2004.
- [19] Dimitris Manolakis, Christina Siracusa, and Gary Shaw. Hyperspectral subpixel target detection using linear mixing model. *IEEE Trans. Geoscience Remote Sensing*, 2001.
- [20] P. Mather. *Land Cover Classification Revisited*, chapter 2, John Wiley & Sons, Inc., U.K., July 1999.
- [21] Robert O. Green, Michael L. Eastwood, Charles M. Sarture, Thomas G. Chrien, Mikael Aronsson, Bruce J. Chipendale, Jessica A. Faust, Betina E. Pavri, Christopher J. Chovit, Manuel Solis, Martin R. Olah, and Orlesa Williams. Imaging spectroscopy and the airborne visible/infrared imaging spectrometer (AVIRIS). *Rem. Sens. of the Environ.*, 1998.
- [22] Eric Moulines, Jean-Francois Cardoso, and Elisabeth Gassiat. Maximum likelihood for blind separation and deconvolution of noisy signals using mixture models. In *Proc. of the IEEE Int. Conf. on Acoustics, Speech, and Signal Processing*, volume 5, 1997.
- [23] J. Pearlman, C. Segal, L. Liao, S. Carman, M. Folkman, B. Browne, L. Ong, and S. Ungar. The HYMAP airborne hyperspectral sensor: The system, calibration and performance. In *Proc. of the 1st EARSEL Workshop on Imaging Spectroscopy*, 1998.
- [24] M. Petrou and P. G. Foschi. Confidence in linear spectral unmixing of single pixels. *IEEE Trans. Geosci. Remote Sensing*, 1999
- [25] L.J. Rickard, R. Basedow, E. Zalewski, P. Silvergate, and M. Landers. HYDICE: An airborne system for hyperspectral imaging. In *Proc. of SPIE*, volume 1937, 1993.
- [26] John A. Richards and Xiuping Jia. *Remote Sensing Digital Image Analysis: An Introduction*. Springer, fourth edition, 2005
- [27] R. Singer. Near-infrared spectral reflectance of mineral mixtures: Systematic combinations of pyroxenes, olivine, and iron oxides. *J. of Geophysical Research*, 86:7967-7982, 1981.
- [28] R. B. Singer and T. B. McCord. Mars: Large scale mixing of bright and dark surface materials and implications for analysis of spectral reflectance. In *Proc. of the 10th Lunar and Planetary Sci. Conf.*, pages 1835-1848, 1979.
- [29] S. G. Ungar, J.S. Pearlman, J.A. Mendenhall, and D. Reuter. Overview of the earth observing one (eo-1) mission. *IEEE Trans. Geoscience Remote Sensing*, 41(6-1):1149-1159, 2003.
- [30] R. Singer. Near-infrared spectral reflectance of mineral mixtures: Systematic combinations of pyroxenes, olivine, and iron oxides. *J. of Geophysical Research*, 86:7967-7982, 1981.
- [31] J. Bioucas-Dias and J. Nascimento, "Hyperspectral subspace identification," *IEEE Trans. Geoscience Remote Sens.*, vol. 46, no. 8, pp. 2435-2445, 2008.
- [32] J. Nascimento and J. Bioucas-Dias, "Vertex component analysis: A fast algorithm to unmix hyperspectral data," *IEEE Trans. Geoscience Remote Sens.*, vol. 43, no. 4, pp. 898-910, 2005.
- [33] J.M. Bioucas-Dias and J. Nascimento, "Hyperspectral unmixing based on mixtures of Dirichlet components," *IEEE Trans. Geoscience Remote Sens.*, vol. 50, no. 3, pp. 863-878, 2012 Available online: <http://speclab.cr.usgs.gov/spectral-lib.html>